

BRIEF REPORT



Virus preparations from the mixed-infected P70 Pinot Noir accession exhibit GLRaV-1/GVA ‘end-to-end’ particles

Antoine Alliaume¹ · Catherine Reinbold¹ · Mathieu Erhardt² · Monique Beuve¹ · Jean-Michel Hily¹ · Olivier Lemaire¹ · Etienne Herrbach¹ Received: 5 June 2018 / Accepted: 1 August 2018 / Published online: 16 August 2018
© Springer-Verlag GmbH Austria, part of Springer Nature 2018

Abstract

P70 is a Pinot Noir grapevine accession that displays strong leafroll disease symptoms. A high-throughput sequencing (HTS)-based analysis established that P70 was mixed-infected by two variants of grapevine leafroll-associated virus 1 (GLRaV-1, genus *Ampelovirus*) and one of grapevine virus A (GVA, genus *Vitivirus*) as well as by two viroids (hop stunt viroid [HSVd] and grapevine yellow speckle viroid 1 [GYSVd1]) and four variants of grapevine rupestris stem pitting-associated virus (GRSPaV). Immunogold labelling using gold particles of two different diameters revealed the existence of ‘hybrid’ particles labelled at one end as GLRaV-1, with the rest labelled as GVA. In this work, we suggest that immunogold labelling can provide information about the biology of the viruses, going deeper than just genomic information provided by HTS, from which no recombinant or ‘chimeric’ GLRaV-1/GVA sequences had been identified in the dataset. Our observations suggest an unknown interaction between members of two different viral species that are often encountered together in a single grapevine, highlighting potential consequences in the vector biology and epidemiology of leafroll and rugose-wood diseases.

Originally, the Pinot Noir P70 accession was a ‘trap-plant’ in a Burgundy vineyard in which many vines showed strong symptoms of leafroll disease. Mature canes were recovered, and replicates of this accession were propagated and maintained in a greenhouse of the INRA research center located in Colmar, Alsace, France. The strong leafroll disease symptomatology observed in the field was reproduced, and greenhouse samples were used as source material for the present study. The P70 accession is known to be coinfecting with grapevine leafroll-associated virus 1 (GLRaV-1) and grapevine virus A (GVA), as established by DAS-ELISA [11]. A recent deep sequencing study revealed P70 to be infected by a total of 11 variants of viruses and viroids: two very distinct

variants of GLRaV-1, one of GVA, four different grapevine rupestris stem pitting-associated virus (GRSPaV) variants, and two variants each of the viroids hop stunt viroid (HSVd) and grapevine yellow speckle viroid 1 (GYSVd1) [1].

Grapevine leafroll-associated virus 1 (GLRaV-1, genus *Ampelovirus*, family *Closteroviridae*) is one of the viruses associated with the ‘grapevine leafroll disease complex’ that is present in all major grape-growing regions worldwide. Leafroll disease affects all grapevine rootstocks and *Vitis vinifera* varieties and is generally associated with a significant decrease in grape and wine quality and yield [12]. Characteristic leaf symptoms appear in summer and fall, with downward rolling of the leaf margin, interveinal reddening in red-berried varieties, and chlorosis in white varieties [12]. Like all members of the family *Closteroviridae*, GLRaV-1 is a phloem-restricted virus that is graft-transmissible. GLRaV-1 and other leafroll ampeloviruses are naturally spread in vineyards by several mealybugs and soft scales [6]. Grapevine virus A (GVA, genus *Vitivirus*, family *Betaflexiviridae*) is associated with ‘Kober stem grooving syndrome’, one of the ‘rugose wood complex’ disorders, which is considered a secondary disease of grapevine [13].

Grapevines with leafroll are frequently coinfecting with phloem-limited vitiviruses, such as GVA [18], which are also transmissible by mealybugs and soft scales. Moreover,

Handling Editor: F. Murilo Zerbini.

Antoine Alliaume and Catherine Reinbold contributed equally to the work.

✉ Olivier Lemaire
olivier.lemaire@inra.fr

¹ SVQV, Université de Strasbourg, INRA, 68000 Colmar, France

² Institut de Biologie Moléculaire des Plantes, CNRS UPR2357, Université de Strasbourg, 67084 Strasbourg, France

since vitiviruses are frequently transmitted along with GLRaVs, the hypothesis that the ampelovirus may assist the coinfecting vitivirus during transmission has been raised [6, 7, 14, 21] and has generated an active debate within the grapevine entomology and virology community [6, 18]. For this work, viral particles were purified from 80 g of P70 accession leaves sampled in greenhouses early in April 2014, following a previously described protocol [1]. Prior to further analysis, virions were kept at -80°C . Immunogold labelling [20] was performed to identify and discriminate between GLRaV-1 virions and GVA particles during virion purification. Briefly, a drop of purified particles was placed on 300-mesh Formvar/carbon-coated grids for 1 h. Then, grids were rinsed with PBS and treated with a blocking buffer (10 mM Tris HCl, 100 nM NaCl, 1% BSA, 0.1% Tween) for 10 min. They were then incubated for 1 h with primary antiserum (1/200 in blocking buffer) (Bioreba AG, Reinach, Switzerland) targeting either GVA or GLRaV-1 particles, either separately or simultaneously at room temperature. After a washing step with TE buffer (10 mM Tris-HCl, pH 7.4, 1 mM EDTA), grids were incubated in blocking buffer for 30 min. Secondary antiserum conjugated with gold particles (1/30 in blocking buffer) was then applied for 1 h at room temperature. Goat anti-mouse antiserum conjugated with 10-nm colloidal gold particles was used to label GLRaV-1 particles, while goat anti-rabbit antiserum conjugated with either 10- or 30-nm colloidal gold particles was used for GVA. Grids were then successively incubated in blocking buffer for 30 min, rinsed with TE buffer and then water, and finally stained with 3% uranyl acetate. The preparations were viewed using a FEI/Philips EM208 transmission electron microscope operating at 80 kV. Film-based images were captured on Kodak Electron Image Film SO-163 (Electron Microscopy Science, Hatfield, PA, USA), developed, and then scanned. From this, GLRaV-1 virions (Fig. 1A) were readily observed by electron microscopy using specific antibodies directed against GLRaV-1 labelled with 10-nm gold particles (@GLRaV-1). While virions completely coated with specific antibodies directed against GLRaV-1 were generally observed (Fig. 1A), some particles were coated only partially (Fig. 1B and C for GLRaV-1 and GVA, respectively). Such partial labelling could possibly be an artefact due to the antibodies not recognizing some variants. However, after incubation in a mixture of both primary antibodies (@GLRaV-1 and @GVA), a large number of ‘doubly labelled’ particles aggregated in an ‘end-to-end’ manner were observed (Fig. 1D) in which one end of the virion (ca. 2/3 of its length) was coated with GLRaV-1-specific antibodies labelled with 10-nm gold particles, and the other (ca. 1/3 of its length) was coated with @GVA with 30-nm gold label. At higher magnification, such aggregates seemed to be seamless (Fig. 1E). It is interesting to note that no complete single GVA particles were ever observed. Only

smaller virions, probably broken particles, and long GVA particles aggregated ‘end-to-end’ were detected.

To confirm our results and reject the hypothesis of an experimental artefact, virion purifications and labelling assays were performed four other times from leaf samples collected from the P70 accession at different times during the growing season (early- and mid-April 2017, May 2017 and late September 2017). Once again, alongside homogeneously and fully gold-labelled virions, we observed partially labelled particles in all purified preparations from samples collected at different times of the year. Particles from one representative immunogold labelling experiment were then measured using a Hitachi h7500 transmission electron microscope operating at 80 kV. Images were taken using a Hamamatsu camera linked to AMT image acquisition and processing software. Particle lengths were measured using Image J software. Five squares of three electron microscopy grids were examined extensively, and from these, all GLRaV-1 particles (> 1000 nm) and ‘chimeric’ particles (with a GLRaV-1 part > 1000 nm) were recorded and measured (Table 1). When considering only largely intact GLRaV-1 particles, the prevalence of such ‘doubly labelled’ particles was found to be close to 20% (Table 1). These ‘end-to-end’ GLRaV-1 and GVA particles followed a perfect continuum without any noticeable break between the ends of the ‘doubly labelled’ particles (Fig. 1B, C, D and E).

Such an aggregation of particles in purified preparations has been described previously for members of various viral species [2, 5, 9, 10, 15]. These ‘end-to-end’ aggregation properties have been used recently in nanotechnology [16, 17, 19] for which specific physical/chemical conditions are required. A possible explanation for our observations could be that the process of assembly of coat protein subunits along the viral RNA of one virus could switch to allow integration of subunits from the other coinfecting virus, thus resulting in virions partially composed of subunits of both viruses, indicating a form of heterologous encapsidation. Heteroencapsidation between two distinct coinfecting viruses has been documented previously for the barley and cereal yellow dwarf viruses (family *Luteoviridae*) and shown to lead to phenotypic changes, especially in aphid vector specificity, as reviewed by Falk and Tian [4]. This has been shown in some other cases to occur between related begomoviruses [8]. Using immunoelectron microscopy (IEM), it has been reported that two coinfecting potyviruses (an aphid-transmissible isolate of papaya ringspot virus and a non-transmissible isolate of zucchini yellow mosaic virus) displayed purified virions that were sectorially labelled with antibodies directed against each virus, indicating that they were chimeric virions composed of subunits of both viruses [3]. To our knowledge, this is the first time that such ‘end-to-end’ particle aggregations between two filamentous viruses belonging to two

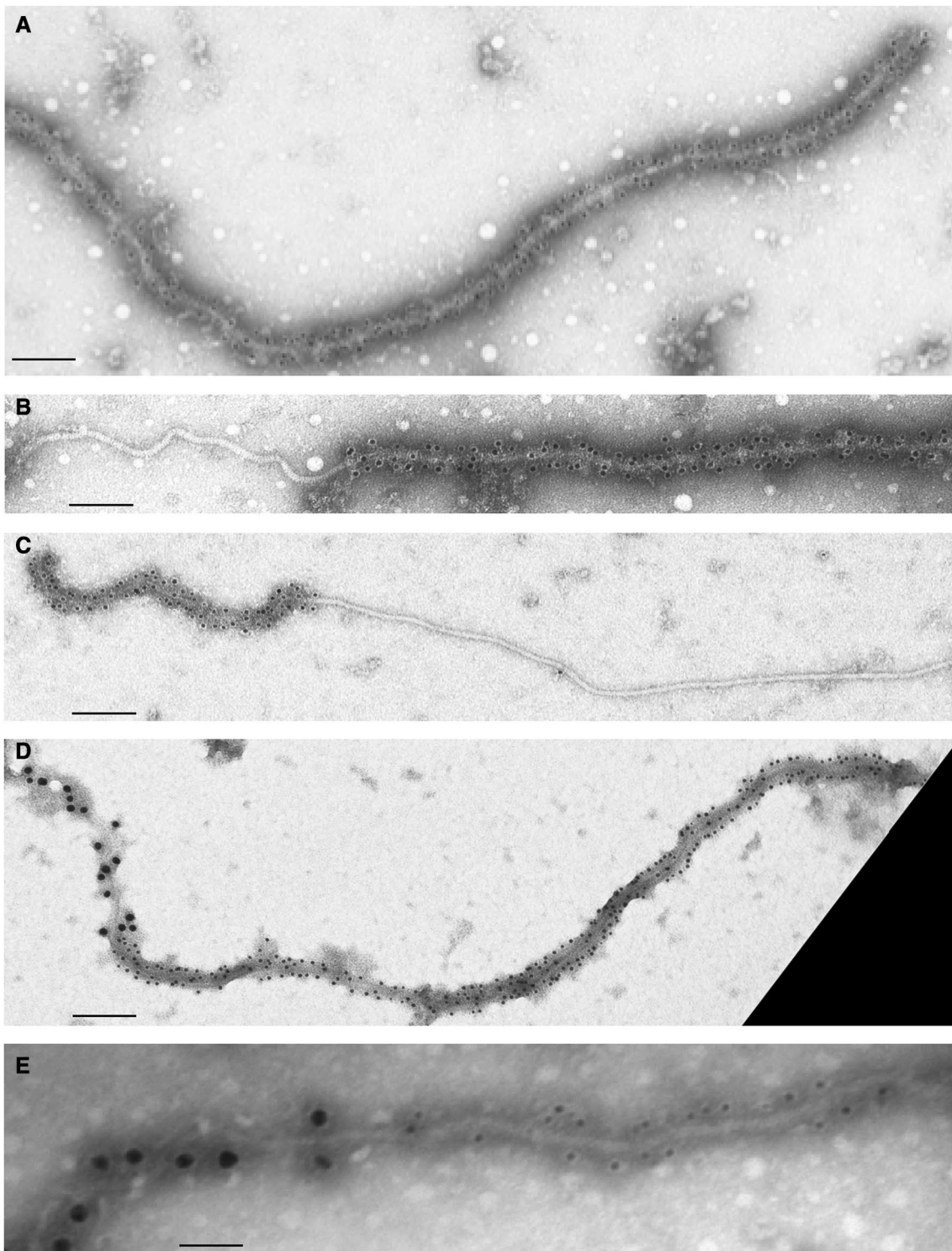


Fig. 1 Immunogold labelling of virions. Immunogold labelling of virions using 10-nm-gold-labelled @GLRaV-1 (A, B), 10-nm-gold-labelled @GVA (C), or an admix of 10-nm-gold-labelled @

GLRaV-1 and 30-nm-gold-labelled @GVA (D, E) Bars: A=160 nm, B=140 nm, C=230 nm, D=260 nm, E=100 nm

distinct families, such as GLRaV-1 and GVA, have been observed. This is quite intriguing, knowing that no 'end-to-end' aggregations between complete GVA particles

were ever visualized in our purifications (*i.e.*, no observation of GVA particles that were longer than expected). The existence of such 'chimeric' GVA/GLRaV-1 particles

Table 1 Measurements of doubly labelled GLRaV-1/GVA particles using Image J software. Five squares of three electron microscopy grids were examined extensively, and from these, all GLRaV-1 particles (> 1000 nm) and ‘chimeric’ GVA/GLRaV-1 particles (with the GLRaV-1 part being > 1000 nm) were recorded and measured

| | | GRID #1 | | | GRID #2 | | | GRID #3 | | |
|------------|-----------|----------------------|-----------|-------------|----------------------|-----------|-------------|----------------------|-----------|-------------|
| | | Particle length (nm) | | | Particle length (nm) | | | Particle length (nm) | | |
| | | Chimeric particles | | | Chimeric particles | | | Chimeric particles | | |
| | | GLRaV-1 | GVA | GLRaV-1 | GLRaV-1 | GVA | GLRaV-1 | GLRaV-1 | GVA | GLRaV-1 |
| Square 1 | Mean | 1371.99 | 721.52 | 1444.86 | 1588.31 | 781.61 | 1255.93 | 1599.85 | 765.10 | 1228.76 |
| | ± SE (nm) | 309.17 | 53.11 | 118.76 | 313.15 | 94.28 | 239.28 | 319.98 | 2.20 | 169.67 |
| | | n=6 | n=2 | | n=29 | n=5 | | n=17 | n=2 | |
| Range (nm) | | (1063-1877) | (683-759) | (1360-1528) | (1206-2307) | (672-899) | (1054-1659) | (1247-2303) | (763-766) | (1108-1348) |
| | | Particle length (nm) | | | Particle length (nm) | | | Particle length (nm) | | |
| | | Chimeric particles | | | Chimeric particles | | | Chimeric particles | | |
| | | GLRaV-1 | GVA | GLRaV-1 | GLRaV-1 | GVA | GLRaV-1 | GLRaV-1 | GVA | GLRaV-1 |
| Square 2 | Mean | 1656.06 | 743.78 | 1075.40 | 1578.09 | 739.66 | 1224.81 | 1503.55 | 820.60 | 1559.85 |
| | ± SE (nm) | 278.81 | 71.70 | 60.62 | 277.82 | 79.52 | 206.19 | 360.66 | 48.03 | 92.44 |
| | | n=15 | n=3 | | n=20 | n=7 | | n=18 | n=4 | |
| Range (nm) | | (1161-2179) | (662-796) | (1005-1116) | (1207-2372) | (654-878) | (1009-1571) | (1028-2412) | (754-858) | (1450-1648) |
| | | Particle length (nm) | | | Particle length (nm) | | | Particle length (nm) | | |
| | | Chimeric particles | | | Chimeric particles | | | Chimeric particles | | |
| | | GLRaV-1 | GVA | GLRaV-1 | GLRaV-1 | GVA | GLRaV-1 | GLRaV-1 | GVA | GLRaV-1 |
| Square 3 | Mean | 1343.62 | | | 1570.92 | 749.62 | 1369.04 | 1569.23 | 752.36 | 1172.93 |
| | ± SE (nm) | 172.39 | | | 301.61 | 23.68 | 392.26 | 299.60 | 72.31 | 107.16 |
| | | n=4 | n=0 | | n=22 | n=7 | | n=26 | n=6 | |
| Range (nm) | | (1190-1499) | | | (1190-2106) | (734-801) | (1049-2020) | (1205-2332) | (631-850) | (1000-1315) |
| | | Particle length (nm) | | | Particle length (nm) | | | Particle length (nm) | | |
| | | Chimeric particles | | | Chimeric particles | | | Chimeric particles | | |
| | | GLRaV-1 | GVA | GLRaV-1 | GLRaV-1 | GVA | GLRaV-1 | GLRaV-1 | GVA | GLRaV-1 |
| Square 4 | Mean | 1369.26 | | | 1372.57 | 795.42 | 1246.49 | 1652.46 | 856.91 | 1386.83 |
| | ± SE (nm) | 229.28 | | | 285.40 | 76.02 | 75.95 | 380.14 | 3.49 | 282.37 |
| | | n=7 | n=0 | | n=17 | n=2 | | n=10 | n=2 | |
| Range (nm) | | (1138-1835) | | | (1044-2072) | (741-849) | (1192-1300) | (1235-2391) | (854-859) | (1187-1586) |
| | | Particle length (nm) | | | Particle length (nm) | | | Particle length (nm) | | |
| | | Chimeric particles | | | Chimeric particles | | | Chimeric particles | | |
| | | GLRaV-1 | GVA | GLRaV-1 | GLRaV-1 | GVA | GLRaV-1 | GLRaV-1 | GVA | GLRaV-1 |
| Square 5 | Mean | 1323.17 | 664.084 | 1698.635 | 1472.22 | 765.19 | 1245.04 | 1562.51 | 819.49 | 1278.40 |
| | ± SE (nm) | 247.10 | | | 292.21 | 40.99 | 227.91 | 162.08 | 14.92 | 186.68 |
| | | n=3 | n=1 | | n=24 | n=8 | | n=12 | n=3 | |
| Range (nm) | | (1065-1558) | | | (1127-2041) | (716-824) | (1064-1770) | (1328-1876) | (803-833) | (1141-1490) |

could give rise to a hypothesis explaining why GVA is most often transmitted by mealybugs along with GLRaV-1, but seldom alone. This suggests that GVA might depend on GLRaV-1 in the source plant in order to be transmitted to a healthy vine [6]. Recently, a synergism between vitiviruses and grapevine leafroll viruses has also been described, with GVA being predominantly associated with GLRaV-1 and -3 [18]. From our HTS dataset, no formation of ‘chimeric’ sequences between GLRaV-1 and GVA was detected, using either direct mapping or the *de novo* assembly method [1]. We also did not find any recombination events between GVA and GLRaV-1 sequences. This observation tends to suggest that our observations of chimeric particles might be due to protein-protein or protein-RNA interactions and represent a form of heterologous encapsidation or end-to-end aggregation rather than interspecies recombination. Heteroencapsidation would then raise questions about phenotypic changes leading to vector specificity, as largely documented for other viruses [3, 4, 8]. Nonetheless, such a phenomenon has never been reported for filamentous viruses belonging to two distinct families, such as GLRaV-1 and GVA. In our study, it is not known whether the doubly labelled virions observed harbor the RNA of GLRaV-1, that of GVA, or both (albeit without any covalent link or recombination, as shown by our sequence analysis). It is also not known whether these virions bear the (still undetermined) viral determinant required for vector transmission of either virus, or of both. However, if the existence of such ‘chimeric’ particles were biologically confirmed, it would have consequences in the vector biology and the epidemiology of leafroll and rugose-wood diseases.

Acknowledgements This work was supported by the Institut National de la Recherche Agronomique (INRA) and partially supported by the Agence Nationale pour la Recherche, ANR Vinobodies contract: ANR-14-CE19-0018-02. JMh was funded by the “Metagenome” (28000225) project gathering three French professional committees for viticulture (Interprofessional Committee of Champagne Wine, CIVC, Epernay; Interprofessional Office of Burgundy Wines, BIVB, Beaune and Interprofessional Committee of Wines from Alsace, CIVA, Colmar) and Moët & Chandon. The authors acknowledge Jacky Misbach and the greenhouse team for technical support, and Lionel Ley and the members of the experimental unit of INRA-Colmar for the production of plants.

Compliance with ethical standards

Conflict of interest The authors declare there are no conflicts of interest.

Research involving human participants and/or animals This research did not involve human participants or animals.

Informed consent This research did not involve human participants or animals. All co-authors consent to the publication.

References

1. Beuve M, Hily JM, Alliaume A, Reinbold C, Le Maguet J, Candresse T, Herrbach E, Lemaire O (2018) A complex virome unveiled by deep sequencing analysis of RNAs from a French Pinot Noir grapevine exhibiting strong leafroll symptoms. *Arch Virol*. <https://doi.org/10.1007/s00705-018-3949-9>
2. Bos L, Huttinga H, Maat DZ (1978) Shallot latent virus, a new carlavirus. *Neth J Plant Pathol* 84:227–237
3. Bourdin D, Lecoq H (1991) Evidence that heteroencapsidation between two potyvirus is involved in aphid transmission of a non-aphid-transmissible isolate from mixed infections. *Phytopathology* 81:1459–1464
4. Falk B, Tian T (1999) Transcapsidation interactions and dependent aphid transmission among luteoviruses, and luteovirus-associated RNAs. In: Smith H, Barker H (eds) *The Luteoviridae*. CAB International, Oxon, pp 125–134
5. Harrison BD, Nixon HL (1959) Separation and properties of particles of Tobacco rattle virus with different lengths. *Microbiology* 21:569–580
6. Herrbach E, Alliaume A, Prator CA, Daane KM, Cooper ML, Almeida RPP (2017) Vector transmission of grapevine leafroll-associated viruses. In: Meng B, Martelli GP, Golino DA, Fuchs M (eds) *Grapevine viruses: molecular biology, diagnostics and management*. Springer International Publishing AG, Cham, pp 483–503
7. Hommay G, Komar V, Lemaire O, Herrbach E (2008) Grapevine virus A transmission by larvae of *Parthenolecanium corni*. *Eur J Plant Pathol* 121:185–188
8. Kanakala S, Jyothisna P, Shukla R, Tiwari N, Veer BS, Swarnalatha P, Krishnareddy M, Malathi VG (2013) Asymmetric synergism and heteroencapsidation between two bipartite begomoviruses, tomato leaf curl New Delhi virus and tomato leaf curl Palampur virus. *Virus Res* 174:126–136
9. Kleczkowski A, Nixon HL (1950) An electron-microscope study of potato virus X in different states of aggregation. *Microbiology* 4:220–224
10. Koganezawa H, Yanase H (1990) A new type of elongated virus isolated from apple trees containing the stem pitting agent. *Plant Dis* 74:610–614
11. Le Maguet J, Beuve M, Herrbach E, Lemaire O (2012) Transmission of six ampeloviruses and two vitiviruses to grapevine by *Phenacoccus aceris*. *Phytopathology* 102:717–723
12. Martelli GP (2014) Grapevine-infecting viruses. *J Plant Pathol* 96:7–8
13. Minafra A, Mawassi M, Goszczynski D, Saldarelli P (2017) Grapevine vitiviruses. In: Meng B, Martelli GP, Golino DA, Fuchs M (eds) *Grapevine viruses: molecular biology, diagnostics and management*. Springer International Publishing AG, Cham, pp 229–256
14. Nakaune R, Toda S, Mochizuki M, Nakano M (2008) Identification and characterization of a new vitivirus from grapevine. *Arch Virol* 153:1827–1832
15. Oster G (1947) Studies on the sonic treatment of tobacco mosaic virus. *J Gen Physiol* 31:89–102
16. Petrova AB, Herold C, Petrov EP (2017) Conformations and membrane-driven self-organization of rodlike FD virus particles on freestanding lipid membranes. *Soft Matter* 13:7172–7187
17. Pokorski JK, Steinmetz NF (2011) The art of engineering viral nanoparticles. *Mol Pharm* 8:29–43
18. Rowhani A, Daubert S, Arnold K, Al Rwahnih M, Klaassen V, Golino D, Uyemoto JK (2018) Synergy between grapevine vitiviruses and grapevine leafroll viruses. *Eur J Plant Pathol* 151:919–925. <https://doi.org/10.1007/s10658-018-1426-7>

19. Sharma KP, Ganai AK, Sen D, Prasad BLV, Kumaraswamy G (2013) Exclusion from hexagonal mesophase surfactant domains drives end-to-end enchainment of rod-like particles. *J Phys Chem B* 117:12661–12668
20. Tian T, Rubio L, Yeh H, Crawford B, Falk B (1999) Lettuce infectious yellows virus: in vitro acquisition analysis using partially purified virions and the whitefly *Bemisia tabaci*. *J Gen Virol* 80:1111–1117
21. Zorloni A, Prati S, Bianco PA, Belli G (2006) Transmission of Grapevine virus A and Grapevine leafroll-associated virus 3 by *Heliococcus bohemicus*. *Plant Pathol* 88:325–328